Controlling phase separation of binary Bose-Einstein condensates via mixed-spin-channel Feshbach resonance

Satoshi Tojo,[1] Yoshihisa Taguchi,[1] Yuta Masuyama,[1] Taro Hayashi,[1] Hiroki Saito,[2] and Takuya Hirano[1]
[1]*Department of Physics, Gakushuin University, Tokyo 171-8588, Japan*
[2]*Department of Engineering Science, University of Electro-Communications, Tokyo 182-8585, Japan*
(Received 23 November 2009; revised manuscript received 14 July 2010; published 14 September 2010)

We investigate controlled phase separation of a binary Bose-Einstein condensate in the proximity of a mixed-spin-channel Feshbach resonance in the $|F=1,m_F=+1\rangle$ and $|F=2,m_F=-1\rangle$ states of ^{87}Rb at a magnetic field of 9.10 G. Phase separation occurs on the lower-magnetic-field side of the Feshbach resonance while the two components overlap on the higher-magnetic-field side. The Feshbach resonance curve of the scattering length is obtained from the shape of the atomic cloud by comparison with the numerical analysis of coupled Gross-Pitaevskii equations.

DOI: 10.1103/PhysRevA.82.033609 PACS number(s): 67.85.−d, 03.75.Kk, 03.75.Mn, 05.30.Jp

I. INTRODUCTION

Ultracold atomic gases provide an attractive testing ground for studying dynamics of multicomponent quantum fluids. It has been shown that dual-species quantum gases [1–3], two-component Bose-Einstein condensates (BECs) comprised of two different hyperfine states [4,5], and spinor BECs with different Zeeman sublevels [6–8] exhibit a rich variety of dynamics. The controllability of the intra- and intercomponent interactions via a Feshbach resonance [9] creates numerous possibilities and enriches the physics of multicomponent quantum fluids.

Miscibility between different components is crucially important to the dynamics of multicomponent systems. Phase separation in immiscible two-component BECs has been studied in Ref. [10]. Immiscible two-component BECs have been predicted to have interface instabilities: the Kelvin-Helmholtz instability in the presence of shear flow [11] and the Rayleigh-Taylor instability [12]. On the other hand, the miscibility between different spin components plays a key role in coherent spin dynamics, such as the Josephson oscillation [13,14], spin echoes [15], the Ramsey interferometer [5], spin entanglement [16,17], and determination of the magnetic ground state of a spinor BEC [18].

Papp *et al.* [2] recently tuned the miscibility in binary BECs of ^{85}Rb-^{87}Rb controlling the intracomponent interaction of ^{85}Rb. The present system differs from that in Ref. [2] in that the miscibility of different spin states of an identical species is controlled by an intercomponent Feshbach resonance. For a binary mixture of two different internal states, the populations of the components can be altered at any stage in an experiment via spin manipulations. Although the Feshbach resonance has been reported on different internal states of an identical species [19–21], control of their miscibility has not been discussed.

The scattering length determines the properties of ultracold collisions [22]. Spectroscopic methods for determination of the scattering length by observation of energy shift have been demonstrated [23–26]. While these methods have advantages in accuracy, they are applicable only to the states between which spectroscopic transition is available. In addition, the spectroscopic methods have a disadvantage for high-density systems, since an energy shift caused by atomic density lowers the precision of the estimation.

In this paper, we control phase separation via a Feshbach resonance between internal spin states, $|F=1,m_F=1\rangle \equiv |1\rangle$ and $|F=2,m_F=-1\rangle \equiv |2\rangle$, of ^{87}Rb. The miscibility of these two components is found to depend sensitively on the strength of the applied magnetic field near the Feshbach resonance. The experimental results are compared with numerical simulations of coupled Gross-Pitaevskii (GP) equations. The excellent agreement between the experimental results and the numerical simulations allows us to estimate the scattering length between the internal states. The experiments and simulations for various values of magnetic field yield the resonance curve of the scattering length near the Feshbach resonance. Thus observation of phase separation dynamics can be used as a method to estimate scattering lengths of multicomponent BECs, which does not rely on spectroscopic transition and can be used in the high-density regime.

This paper is structured as follows. In Sec. II, we introduce the mean-field formalism for a binary BEC. In Sec. III, our experimental apparatus and conditions are described. In Sec. IV, experimental results are compared with numerical simulations. Section V is devoted to the conclusions.

II. TWO-COMPONENT CONDENSATES

The dynamics of a binary BEC with inelastic two-body losses is described by coupled GP equations [4,5,18],

$$i\hbar\frac{\partial\psi_1}{\partial t}=\left(-\frac{\hbar^2\nabla^2}{2m}+V+\tilde{g}_{11}|\psi_1|^2+\tilde{g}_{12}|\psi_2|^2\right)\psi_1, \quad (1a)$$

$$i\hbar\frac{\partial\psi_2}{\partial t}=\left(-\frac{\hbar^2\nabla^2}{2m}+V+\tilde{g}_{22}|\psi_2|^2+\tilde{g}_{12}|\psi_1|^2\right)\psi_2, \quad (1b)$$

where ψ_i is the macroscopic wave function for the $|i\rangle$ state, m is the mass of ^{87}Rb, and V is the trap potential. The interaction coefficient is given by $\tilde{g}_{ij}=g_{ij}-i\hbar K_{ij}/2$ with $g_{ij}=4\pi\hbar^2 a_{ij}/m$, where a_{ij} is the scattering length and K_{ij} is the two-body inelastic collision rate between the $|i\rangle$ and $|j\rangle$ states of condensates. The scattering lengths of ^{87}Rb have almost the same values: $a_{22}=95.00a_{\mathrm{B}}$, $a_{11}=100.4a_{\mathrm{B}}$, and $a_{12}=97.66a_{\mathrm{B}}\equiv a_{\mathrm{bg}}$, where a_{B} is the Bohr radius [4]. The scattering lengths determine the miscibility of the binary BEC. The phase separation condition in a uniform system is given by

$a_{12}^2 > a_{11}a_{22}$. The atom density in two-component condensates decreases by the two-body inelastic collisions as

$$\frac{\partial n_m}{\partial t} = -K_{mm} n_m^2 - K_{mm'} n_m n_{m'}. \quad (2)$$

The two-body inelastic collision rates in the $F = 2$ manifold were measured in Ref. [18], giving $K_{22} = 1.04 \times 10^{-13}$ cm^3/s. The two-body inelastic loss in the $F = 1$ manifold is negligible and we assume $K_{11} = 0$.

Near the magnetic Feshbach resonance, the intercomponent interaction $\tilde{g}_{12}$ is changed. The interspecies scattering length in a complex form can be expressed as a Lorentzian function [27]. Since the imaginary part of the scattering length is incorporated in K_{12}, we use the effective scattering length between the $|1\rangle$ and $|2\rangle$ states defined by

$$a_{12}^{\rm eff} \equiv a_{\rm bg} + \Delta a(B) = a_{\rm bg}\left(1 - \frac{\Delta B(B - B_0)}{(B - B_0)^2 + (\gamma_{\rm B}/2)^2}\right), \quad (3)$$

where the parameters B_0, ΔB, and $\gamma_{\rm B}$ are determined later.

III. EXPERIMENT

Our experimental apparatus and procedure used to create ^{87}Rb condensates are the same as those described in Refs. [14,18] except for irradiation of a two-photon $\pi/2$ pulse between the hyperfine states. A BEC containing 10^6 atoms in the $|2,2\rangle$ state is created by evaporative cooling with frequency sweeping of an rf field for 18 s in a magnetic trap. The BEC is loaded into a crossed far-off-resonant optical trap (FORT) at a wavelength of 850 nm and 3×10^5 atoms remain in the FORT. The potential depth of the crossed FORT is estimated to be about 1 μK and the radial (axial) trap frequency is measured to be 141 Hz (21 Hz) using the parametric resonance. After sudden inversion of the quantization axis, the $|2,-2\rangle$ state is transferred to the $|2,-1\rangle \equiv |2\rangle$ state by inducing the Landau-Zenner transition using rf irradiation with an external magnetic field of 20.5 G. Half the atoms in the $|2\rangle$ state are then transferred to the $|1,1\rangle \equiv |1\rangle$ state by irradiation of a $\pi/2$ pulse of the rf and microwave field for 5 ms. After time evolution for $t_{\rm ev}$ in a precisely controlled magnetic field $B_{\rm ev}$, the crossed FORT is turned off. The magnetic field is kept on for the first 5 ms of the time of flight (TOF) to maintain the scattering length during expansion of the atomic cloud. After applying a Stern-Gerlach pulse, absorption images are obtained. In order to take the image of each component, we apply a sequence of two short pulses after TOF times of 15 ms for $F = 2$ and 18 ms for $F = 1$ with repumping to $F = 2$. The fluctuation in the number of atoms is estimated to be 10%. The relative population fluctuates between 0.45 and 0.55 in each run of the experiment [18,28].

The magnetic-field strength of the Feshbach resonance can be determined by measuring the atomic losses. In our experimental conditions, atomic losses by one- and three-body inelastic collisions are negligible compared with that by two-body inelastic collisions [18]. The total number of atoms in the $|2\rangle$ state decreases rapidly with increasing trap time $t_{\rm ev}$ because of hyperfine-changing inelastic collisions such as $|2,-1\rangle$, $|2,-1\rangle \rightarrow |1,m_F\rangle, |1 \text{ or } 2,m'_F\rangle$ and $|2,-1\rangle, |1,-1\rangle \rightarrow |1,m_F\rangle$, $|1,m'_F\rangle$. For a magnetic field far from the Feshbach resonance, the two-body inelastic collision rate between the $|2\rangle$ and $|1\rangle$ states is estimated to be $K_{12} = 0.5 \times 10^{-13}$ cm^3/s, which is obtained by comparing the atom loss in our experiment and a solution of the GP equation (1). Both the elastic scattering length and the inelastic collision loss rate are altered in the vicinity of the Feshbach resonance [9]. Figure 1(a) shows the total number of atoms after the TOF for evolution times $t_{\rm ev}$ of 25, 50, and 75 ms. For $t_{\rm ev} = 25$ ms, density profiles were almost the same at both lower and higher-magnetic-field near the Feshbach resonance. We estimated K_{12} for $t_{\rm ev} =$ 25 ms by solving Eq. (2) numerically with the single-mode approximation. The uncertainty arises from the fluctuation in the initial number of atoms. The data are fitted by a Lorentzian function as shown in Fig. 1(b), which gives a Feshbach resonance field B_0 to be 9.100 G and $\gamma_{\rm B}$ to be 30 mG. The fluctuation in the magnetic field $B_{\rm ev}$ is estimated to be less than 5 mG by observing the magnetic dipole transitions, and the residual gradient magnetic field is estimated to be 30 mG/cm [14]. The magnetic-field strength is calibrated by Rabi spectra between clock states with the microwave irradiation. The uncertainty in this calibration is 5 mG. The resonant magnetic field obtained in our experiment, 9.100(5) G, agrees with the theoretical prediction [29] within the experimental uncertainty.

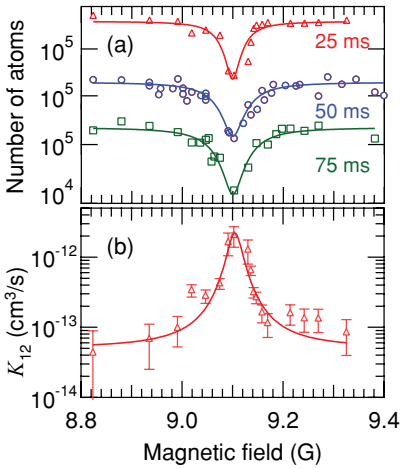

FIG. 1. (Color online) (a) Magnetic-field dependence of the atom number for evolution times $t_{\rm ev}$ of 25, 50, and 75 ms. (b) Inelastic collision rate estimated by Eq. (2) at $t_{\rm ev} = 25$ ms. Solid lines are Lorentzian functions fit to the data with a center at 9.10 G.

IV. RESULTS AND DISCUSSION

The column densities of the binary BEC around the Feshbach resonance for $t_{\rm ev} = 75$ ms are shown in Fig. 2. At a magnetic field far from the Feshbach resonance ($B_{\rm ev} = 8.30$ and 10.05 G), the two components exhibit phase separation [4,5]. The domain structure of phase separation depends not only on the scattering lengths but also on the number of atoms and the relative populations. The scattering lengths and inelastic collision rates for $B_{\rm ev} = 8.30$ G and those for $B_{\rm ev} = 10.05$ G are almost the same, since their density patterns are similar. The behaviors of the binary BEC in the vicinity of the Feshbach resonance at 9.10 G change dramatically in Fig. 2 due to the change in the scattering length and the inelastic collision rate. The domain structures on the lower-magnetic-field side near the Feshbach resonance ($B_{\rm ev} = 9.05$ and 9.08 G)

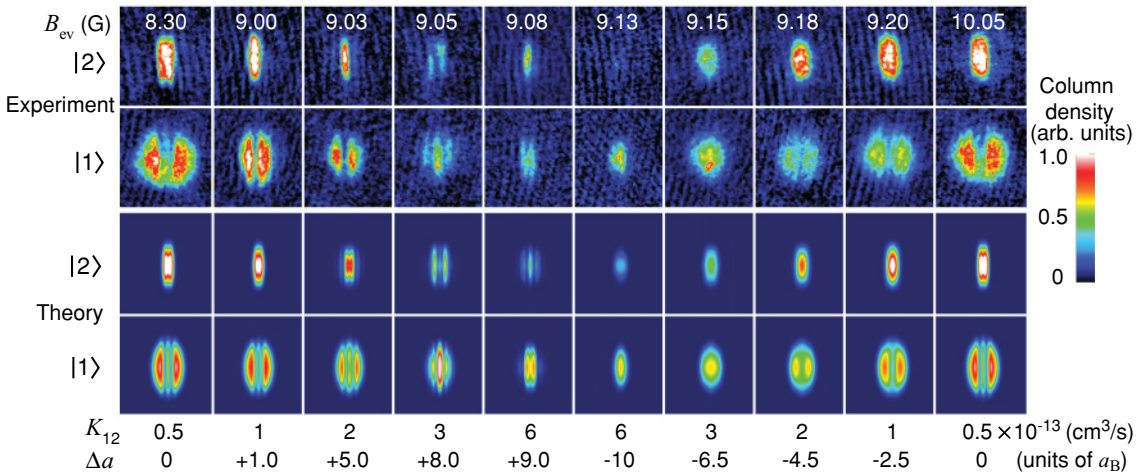

FIG. 2. (Color online) Column densities of the $|2\rangle$ and $|1\rangle$ states obtained by the experiment (upper panels) and the numerical simulation (lower panels) as a function of magnetic field B_{ev}. The field of the view is 316 (vertical) × 290 μm (horizontal). The two-body inelastic collision rates K_{12} (10^{-13} cm^3/s) and the change in the scattering lengths Δa used in the numerical simulation are indicated at the bottom.

are quite different from that at $B_{ev} = 8.30$ G. On the other hand, the domain structure disappears at higher-magnetic-fields around the Feshbach resonance. The behavior at 9.15 G is quite different from that at 9.05 G even though the numbers of atoms are almost the same. These results indicate that the scattering length a_{12} significantly changes at $B_{ev} \simeq 9.1$ G. The domain structures depicted in Fig. 2 are reproducible within the experimental fluctuations in the initial number of atoms and the relative populations.

We numerically solve coupled GP equations (1) for various values of Δa and K_{12}, and we obtain the column densities of atomic clouds after the TOF (lower panels of Fig. 2). The GP equations were solved by the Crank-Nicolson method. The numerically obtained column densities are smoothed to account for the spatial resolution (3.2 μm) of the CCD camera. The values of Δa and K_{12} are determined as follows. First, we assume $\Delta a = 0$ and calculate the time evolution of the number of atoms for various K_{12} using the coupled GP equations (1). We then compare the results with the experimental ones and estimate the value of K_{12}. We confirmed that the difference between the number of atoms for $\Delta a = 0$ and that for $\Delta a \neq 0$ is less than 15%, which is comparable to the fluctuation in the initial number of atoms and does not affect the estimation of K_{12}. We next calculate the column densities for various values of Δa, compare them with the experimental results, and estimate the value of Δa. For example, Fig. 3 shows a catalog of the column densities for $K_{12} = 3 \times 10^{-13}$ cm^3/s, which corresponds to $B_{ev} = 9.05$ and 9.15 G in Fig. 2. Comparing the experimental column densities in Fig. 2 with numerical ones in Fig. 3, we can estimate scattering lengths. We assume that the most probable scattering length minimizes the root-mean-square deviation $s = 1/2 \sum_{m=1}^{2} \sqrt{\sum_{j=1}^{N} [\alpha_{\mathrm{expt}}^{(m)}(z_j) - \alpha_{\mathrm{calc}}^{(m)}(z_j)]^2 / N}$, where $\alpha_{\mathrm{expt}}^{(m)}(z)$ and $\alpha_{\mathrm{calc}}^{(m)}(z)$ are optical densities of the mth component in an experiment and a calculation at z, respectively. Figure 4 shows integrated optical densities obtained by the experiment at 9.05 G and numerical calculation at $\Delta a = 7.5 a_B$, $8.0 a_B$, and $8.5 a_B$. We find that the phase-separation dynamics is sensitive to the change in the scattering length by $0.50 a_B$. The differences between experiments and calculations are expressed by s values as shown in Fig. 5. The value of Δa that minimizes the value of the root-mean-square deviation $s_{\min}$ is $\Delta a = 8.0 a_B$ for $B_{ev} = 9.05$ G. In the range of $\Delta a > 8.0 a_B$, fluctuation of s is expected to be larger than that in $\Delta a < 8.0 a_B$. This is because the density distribution of each component forms complex structures at $\Delta a > 8.0 a_B$ while it shows simple domain structure in $\Delta a < 8.0 a_B$. The phase-separation dynamics can thus be used as a probe for estimating the scattering length in a binary BEC.

The density patterns are sensitive to the differences in the scattering length for positive Δa. The accuracy of the estimated scattering lengths is therefore typically $\pm 1 a_B$ for $\Delta a \gtrsim 3 a_B$. However, in the close vicinity of the Feshbach resonance, the domain structure becomes moderate since the number of atoms decreases considerably, which makes accurate estimation of Δa difficult. For $-7 a_B \lesssim \Delta a < 0$ in Fig. 3, an inhomogeneous density distribution is formed, even though the phase-separation condition is not satisfied; we can estimate $\Delta a = -6.5 a_B$ at $s_{\min}$ for $B_{ev} = 9.15$ G. This is

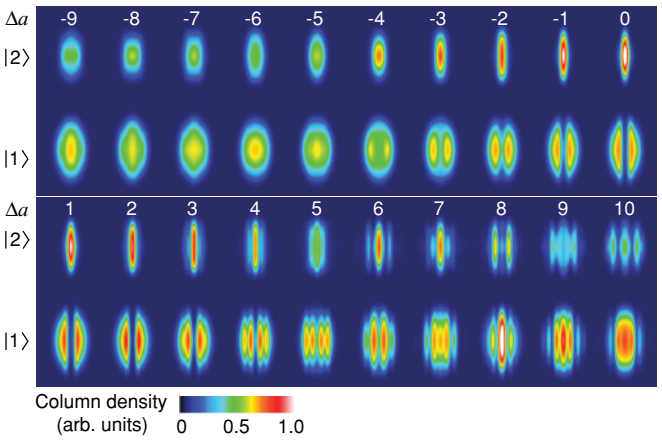

FIG. 3. (Color online) Numerically obtained column density distributions for various scattering lengths at an evolution time of 75 ms with $K_{12} = 3 \times 10^{-13}$ cm^3/s. The relative scattering length Δa in units of a_B is indicated in the top row.

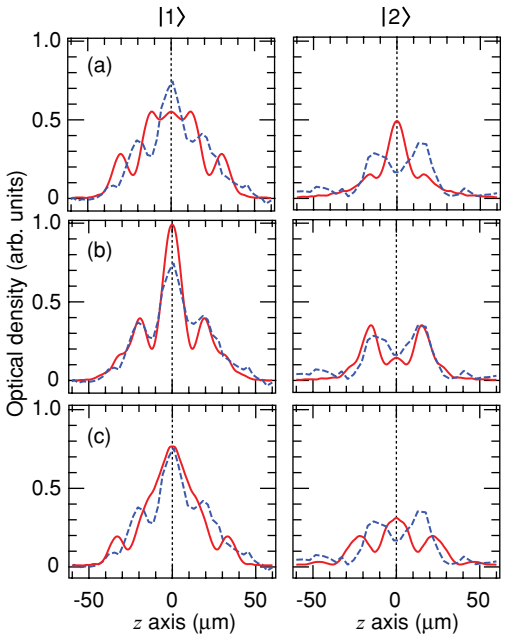

FIG. 4. (Color online) Comparison between the experimentally observed density distributions at $B_{ev} = 9.05$ G (dashed lines) and numerical ones (solid lines) obtained for (a) $\Delta a = 7.5a_B$, (b) $8.0a_B$, and (c) $8.5a_B$.

because the number of $|2\rangle$ atoms decreases rapidly, giving rise to a nonequilibrium density distribution. Clear phase separation is necessary for precise estimation of the scattering length between $|1\rangle$ and $|2\rangle$. In our experiment, $t_{ev} < 25$ ms is insufficient for observing the phase separation. For $t_{ev} > 100$ ms, the number of atoms in the $|2\rangle$ state becomes too small to estimate Δa. The evolution time of $t_{ev} = 75$ ms is the most suitable to estimate the scattering length.

For a uniform system, the Bogoliubov excitation spectrum has the form [30]

$$(\hbar\omega)^2 = \varepsilon\left[\varepsilon + g_{11}n_1 + g_{22}n_2 \pm \sqrt{(g_{11}n_1 - g_{22}n_2)^2 + 4n_1n_2g_{12}^2}\right], \quad (4)$$

where $n_j = |\psi_j|^2$ is the atom density and $\varepsilon = \hbar^2k^2/(2m)$ with k being the excitation wave number. When $g_{12}^2 > g_{11}g_{22}$,

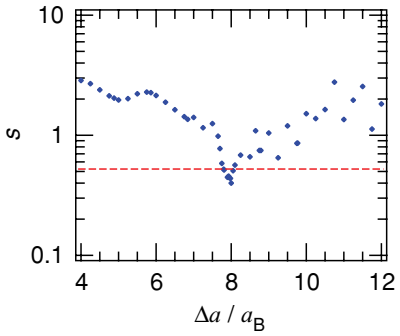

FIG. 5. (Color online) Root-mean-square deviation between experiments and calculations at 9.05 G with $K_{12} = 3 \times 10^{-13}$ cm^3/s. The dashed line shows $1.3s_{min}$, which is defined as a threshold for determination of the error bar of the scattering length.

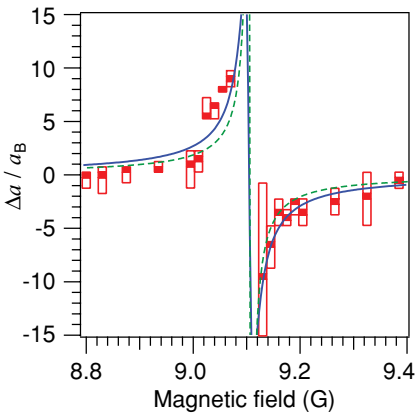

FIG. 6. (Color online) Estimated value of the change in the scattering length between the $|1\rangle$ and $|2\rangle$ states for a magnetic field around the Feshbach resonance. The scattering lengths at s_{min} are shown as filled squares and fitted by Eq. (3) (solid curve). The open squares correspond to s below the threshold value of $1.3s_{min}$. The theoretical prediction in Ref. [29] is indicated by the dashed curve.

ω is imaginary for $\varepsilon < [(g_{11}n_1 - g_{22}n_2)^2 + 4n_1n_2g_{12}^2]^{1/2} - (g_{11}n_1 + g_{22}n_2)$ and the system becomes dynamically unstable against phase separation. The exponential growth of the unstable mode is approximately given by

$$\exp\left(\int dt\, \mathrm{Im}\omega(t)\right), \quad (5)$$

where $\omega(t)$ depends on time since n_1 and n_2 decrease with time. The wavelength that maximizes Eq. (5) is most unstable; for example, it is estimated to be 8.9 μm for $K_{12} = 1 \times 10^{-13}$ cm^3/s and $\Delta a = 1.0a_B$, corresponding to 9.00 G, and 4.9 μm for $K_{12} = 3 \times 10^{-13}$ cm^3/s and $\Delta a = 8.0a_B$, corresponding to 9.05 G in Fig. 2, respectively. These estimations of the most unstable wavelengths are in good agreement with the numerical solutions of Eq. (1) before the TOF. By the TOF expansion, the wavelengths in the density pattern become a few times larger.

Figure 6 depicts the normalized scattering length Δa. The theoretical prediction in Ref. [29] is shown as the dashed curve. The scattering lengths are obtained by the method in Fig. 5. The filled squares correspond to s_{min} and the open squares show accuracy ranges below $1.3s_{min}$ of the threshold. They are best fitted by Eq. (3) (solid line) with $B_0 = 9.104$ G ($\gamma_B = 13$ mG, $\Delta B = 3$ mG). The value of ΔB is in good agreement with that of the theoretical prediction and other experiments [19–21,29]. The discrepancy in γ_B may be caused by uncertainties near the resonance field.

The accuracy of Δa in our method is comparable to that in the method using the Ramsey fringe [21]. At $B_{ev} > B_0$ in the high-density regime, the accuracy of Δa in our method is improved at large Δa because the phase-separation dynamics is sensitive to Δa. On the other hand, the accuracy in the Ramsey fringe method at large Δa becomes worse owing to density inhomogeneity caused by dramatic phase separation. We note that the discrepancies in the scattering length between experimental estimation and theoretical prediction may be caused by entangled spin states or molecular states near the

Feshbach resonance [16,17]. If these effects are taken into account, the accuracy of the method may be improved.

V. CONCLUSIONS

In conclusion, we observed the time evolution of binary ^{87}Rb condensates in the $|2,-1\rangle$ and $|1,1\rangle$ hyperfine states around the Feshbach resonance at 9.10 G. In the vicinity of the Feshbach resonance, the miscibility of the two components is tuned to be both immiscible and miscible. Phase separation occurs on the lower-field side of the Feshbach resonance, while miscible behavior is observed on the higher-field side. We performed numerical simulations using coupled GP equations and proposed a method for determination of the scattering length. We estimated the values of Δa and K_{12} by comparing the experimental and numerical density distributions of the atomic cloud. From systematic experiments and simulations, we obtained the resonance curve of scattering length around the Feshbach resonance.

Our method for determination of the scattering length can be used for not only spectroscopic states but also nonspectroscopic states, and it is powerful technique for the high-density regime in both identical and different isotopes. Miscibility control via a mixed-spin-channel Feshbach resonance will open up new possibilities for multicomponent quantum fluids, such as controlled quantum phase transition between miscible and immiscible phases with precise tuned scattering lengths. In addition, this technique can be applied for a precise measurement of a magnetic field below submilligauss range in cases when the scattering length curves are well known.

ACKNOWLEDGMENTS

We would like to thank T. Kuwamoto, T. Tanabe, K. Hamazaki, M. Iwata, and E. Inoue for their experimental assistance. We also thank M. Tsubota for valuable discussions. This work was supported by the Sumitomo Foundation, Grants-in-Aid for Scientific Research (No. 17071005, No. 18684024, No. 19740248, No. 20540388, and No. 22340116) from the Ministry of Education, Culture, Sports, Science, and Technology of Japan, and the Japan Society for the Promotion of Science (JSPS) through its Funding Program for World-Leading Innovative R&D on Science and Technology (FIRST Program).

[1] G. Modugno, M. Modugno, F. Riboli, G. Roati, and M. Inguscio, Phys. Rev. Lett. **89**, 190404 (2002).
[2] S. B. Papp, J. M. Pino, and C. E. Wieman, Phys. Rev. Lett. **101**, 040402 (2008).
[3] S. Ospelkaus, C. Ospelkaus, L. Humbert, K. Sengstock, and K. Bongs, Phys. Rev. Lett. **97**, 120403 (2006).
[4] D. S. Hall, M. R. Matthews, J. R. Ensher, C. E. Wieman, and E. A. Cornell, Phys. Rev. Lett. **81**, 1539 (1998); K. M. Mertes, J. W. Merrill, R. Carretero-González, D. J. Frantzeskakis, P. G. Kevrekidis, and D. S. Hall, *ibid.* **99**, 190402 (2007).
[5] R. P. Anderson, C. Ticknor, A. I. Sidorov, and B. V. Hall, Phys. Rev. A **80**, 023603 (2009).
[6] J. Stenger, S. Inouye, D. M. Stamper-Kurn, H.-J. Miesner, A. P. Chikkatur, and W. Ketterle, Nature (London) **396**, 345 (1998).
[7] H.-J. Miesner, D. M. Stamper-Kurn, J. Stenger, S. Inouye, A. P. Chikkatur, and W. Ketterle, Phys. Rev. Lett. **82**, 2228 (1999).
[8] D. M. Stamper-Kurn, H.-J. Miesner, A. P. Chikkatur, S. Inouye, J. Stenger, and W. Ketterle, Phys. Rev. Lett. **83**, 661 (1999).
[9] S. Inouye, M. R. Andrews, J. Stenger, H.-J. Miesner, D. M. Stamper-Kurn, and W. Ketterle, Nature (London) **392**, 151 (1998).
[10] T. L. Ho and V. B. Shenoy, Phys. Rev. Lett. **77**, 3276 (1996); B. D. Esry, C. H. Greene, J. P. Burke Jr., and J. L. Bohn, *ibid.* **78**, 3594 (1997); E. Timmermans, *ibid.* **81**, 5718 (1998); H. Pu and N. P. Bigelow, *ibid.* **80**, 1130 (1998).
[11] H. Takeuchi, N. Suzuki, K. Kasamatsu, H. Saito, and M. Tsubota, Phys. Rev. B **81**, 094517 (2010).
[12] K. Sasaki, N. Suzuki, D. Akamatsu, and H. Saito, Phys. Rev. A **80**, 063611 (2009); S. Gautam and D. Angom, *ibid.* **81**, 053616 (2010).
[13] M.-S. Chang, Q. Qin, W. Zhang, L. You, and M. S. Chapman, Nature Phys. **1**, 111 (2005).
[14] T. Kuwamoto, K. Araki, T. Eno, and T. Hirano, Phys. Rev. A **69**, 063604 (2004).
[15] M. Yasunaga and M. Tsubota, Phys. Rev. Lett. **101**, 220401 (2008).
[16] N. Teichmann and C. Weiss, Eur. Phys. Lett. **78**, 10009 (2007).
[17] C. Gross, T. Zibold, E. Nicklas, J. Estève, and M. K. Oberthaler, Nature (London) **464**, 1165 (2010).
[18] S. Tojo, T. Hayashi, T. Tanabe, T. Hirano, Y. Kawaguchi, H. Saito, and M. Ueda, Phys. Rev. A **80**, 042704 (2009).
[19] E. G. M. van Kempen, S. J. J. M. F. Kokkelmans, D. J. Heinzen, and B. J. Verhaar, Phys. Rev. Lett. **88**, 093201 (2002).
[20] M. Erhard, H. Schmaljohann, J. Kronjäger, K. Bongs, and K. Sengstock, Phys. Rev. A **69**, 032705 (2004).
[21] A. Widera, O. Mandel, M. Greiner, S. Kreim, T. W. Hänsch, and I. Bloch, Phys. Rev. Lett. **92**, 160406 (2004).
[22] J. Weiner, V. S. Bagnato, S. Zilio, and P. S. Julienne, Rev. Mod. Phys. **71**, 1 (1999).
[23] J. L. Roberts, N. R. Claussen, J. P. Burke Jr., C. H. Greene, E. A. Cornell, and C. E. Wieman, Phys. Rev. Lett. **81**, 5109 (1998); J. L. Roberts, N. R. Claussen, S. L. Cornish, and C. E. Wieman, *ibid.* **85**, 728 (2000); D. M. Harber, H. J. Lewandowski, J. M. McGuirk, and E. A. Cornell, Phys. Rev. A **66**, 053616 (2002).
[24] C. A. Regal and D. S. Jin, Phys. Rev. Lett. **90**, 230404 (2003).
[25] A. Widera, F. Gerbier, S. Fölling, T. Gericke, O. Mandel, and I. Bloch, New J. Phys. **8**, 152 (2006).
[26] A. Yamaguchi, S. Uetake, S. Kato, H. Ito and Y. Takahashi, New. J. Phys. (to be published).
[27] T. Köhler, K. Goral, and P. S. Julienne, Rev. Mod. Phys. **78**, 1311 (2006); J. M. Hutson, New J. Phys. **9**, 152 (2007).
[28] S. Tojo, A. Tomiyama, M. Iwata, T. Kuwamoto, and T. Hirano, Appl. Phys. B **93**, 403 (2008).
[29] A. M. Kaufman, R. P. Anderson, T. M. Hanna, E. Tiesinga, P. S. Julienne, and D. S. Hall, Phys. Rev. A **80**, 050701(R) (2009).
[30] C. J. Pethick and H. Smith, *Bose-Einstein Condensation in Dilute Gases* (Cambridge University Press, Cambridge, 2002), Sec. 12.